

Article

Species- and Elevation-Dependent Growth Responses to Climate Warming of Mountain Forests in the Qinling Mountains, Central China

Bo Liu ^{1,2}, Eryuan Liang ^{3,4,*} , Kang Liu ^{1,2} and J. Julio Camarero ⁵ 

¹ Shaanxi Key Laboratory of Earth Surface System and Environmental Carrying Capacity, Northwest University, Xi'an 710127, China; liubo@nwu.edu.cn (B.L.); 20132381@nwu.edu.cn (K.L.)

² College of Urban and Environmental Sciences, Northwest University, Xi'an 710127, China

³ Key Laboratory of Alpine Ecology and Biodiversity, Institute of Tibetan Plateau Research, Chinese Academy of Science, Beijing 100101, China

⁴ CAS Centre for Excellence in Tibetan Plateau Earth Sciences, Beijing 100101, China

⁵ Instituto Pirenaico de Ecología (IPE-CSIC), Avda. Montañana 1005, 50192 Zaragoza, Spain; jjcamarero@ipe.csic.es

* Correspondence: liangey@itpcas.ac.cn; Tel.: +86-010-8409-7069

Received: 9 April 2018; Accepted: 2 May 2018; Published: 4 May 2018



Abstract: Climate warming is significantly affecting the composition and function of forest ecosystems. However, the forest responses to climate change in sub-humid and temperate areas are understudied compared with cold and semi-arid areas. Here, we investigate the radial-growth responses of two subalpine conifer species along an elevational gradient located in the Qinling Mountains, a sub-humid and temperate area situated in central China. Three sites dominated by larch (*Larix chinensis* Beissn.) and two other sites dominated by fir (*Abies fargesii* Franch.) located at different elevations were sampled. *L. chinensis* at a higher elevation showed more common and stronger climatic signals than *A. fargesii* at a lower elevation. The radial growth of *L. chinensis* was limited by low pre-growing season temperatures and showed an increasing growth trend in the last few years. On the other hand, *A. fargesii* growth was limited by summer water shortage and it was characterized by a declining trend in the most recent decade. Consequently, *L. chinensis* would benefit from climate warming, whereas *A. fargesii* could be regarded as a vulnerable tree species to warming-induced drought stress.

Keywords: climate warming; dendroecology; temperate forests; tree rings

1. Introduction

Global warming has been significantly influencing the composition, structure, and dynamics of forest ecosystems during the last decades [1,2]. It has been reported that forests are subjected to an increasing risk of growth decline, canopy dieback, and mortality under warming-induced drought stress in semi-arid areas [3–6], but on the other hand, climate warming has increased tree growth and recruitment in cold biomes [7,8]. However, the climate-growth relationship seems to be more complex in humid and sub-humid mountainous areas [9–11], where forest dieback and mortality episodes have been also recorded [2]. Temperate humid and sub-humid forests contribute to ca. 25% of the world's total forest cover and contain about 11% of the vegetation carbon stocks [12]. In light of the critical role played by these forests in the global carbon cycle, it is necessary to have a better understanding of their growth responses to climate warming.

Mountain forests offer a wide range of ecological and socio-economic services. There is growing evidence that these biomes are experiencing more rapid changes in temperature at high rather than low

elevations [7]. In particular, elevational gradients can be used as space-for-time substitutes to assess the influences of climate change on these forest ecosystems [13,14]. At high elevations, global warming tends to increase radial growth, as observed in southeast Tibet [8], the Tianshan Mountains [15], the Iranian Plateau [16], and western N. America [7]. Moreover, the effects of climate on growth depend on species-specific tree traits such as drought tolerance, leaf features, tree size, and wood density, etc. [17–19]. However, it is still less known how the radial-growth responses to climate of different tree species change at different elevations.

Here, we focus on studying the radial-growth responses to climate along elevational gradients of two conifers with different traits. We sampled forests in the Qinling Mountains, which is the highest range located in central China and represents a critical biogeographical boundary for climate and vegetation due to its west-to-east alignment. In these humid mountains, forests are dominated by two conifers, the deciduous larch (*Larix chinensis* Beissn.) and the evergreen fir (*Abies fargesii* Franch.) [20,21]. As reported before, the growth of these two conifers and other conifer species found at different elevations and topographical aspects in the Qinling Mountains is influenced by different climatic factors [20,21]. During the past five decades, there has been a warming trend in this area [22,23]. A continuing warming in association with a declining trend in precipitation decrease might negatively influence the radial growth of mountain conifer forests in this range. However, it is unknown whether warming and drying climatic conditions are significantly affecting long-term growth trends of forests and if elevation influences these responses in such humid environments.

The objectives of this study are: (1) to explore the dominant climatic factors limiting the radial growth of *L. chinensis* and *A. fargesii* across a 500-m elevation gradient (3360–2860 m) located in the Qinling Mountains; and (2) to assess if there are elevation- and species-dependent growth responses to climatic change. We hypothesize that the two study species will show species and elevation-dependent growth responses to global warming. The results will contribute additional knowledge on how mountain forests under humid and temperate conditions are responding to recent global warming.

2. Material and Methods

2.1. Study Area and Climate Data

The Qinling Mountains (32°30' N–34°45' N, 104°30' E–112°45' E) represent a prominent topographic barrier for north- and southward movement of air masses due to their high elevations and west-to-east arrangement. The study area is located in the north aspect of the highest peak in this range (Mt. Taibai, 33°57' N, 107°45' E, 3771.2 m a.s.l.), where an alpine treeline is formed. This area is characterized by temperate and humid to semi-humid climate conditions. As shown by the instrumental records from the meteorological station located in Meixian (34°16' N, 107°44' E, 518 m a.s.l.), the annual mean precipitation and temperature were 592 mm and 13.0 °C from 1960 to 2015, respectively (Figure 1).

In order to test the representativeness of climatic records in Meixian in the study area, we further compared temperature/precipitation variations in Meixian and CRU data and TRMM precipitation. The Climate Research Unit (CRU TS 4.01, 0.5° × 0.5°) monthly air temperature and precipitation from 1960 to 2015 close to the study sites were obtained from <https://crudata.uea.ac.uk/cru/data/hrg/>. The 0.25° × 0.25° gridded TRMM monthly precipitation data from 1998 to 2015 covering the study area were derived from https://disc.gsfc.nasa.gov/datasets/TRMM_3B43_V7/summary. Monthly records in Meixian showed a significant positive correlation with CRU and TRMM data ($p < 0.001$ for all correlations between months). Considering that a calibration for tree growth climate relationships mainly focused on the variability rather than on absolute values, the variations of temperature and precipitation records in Meixian are confident indicators of the conditions in the study area. Due to a shorter period of TRMM data and coarser resolution of CRU data, here we selected monthly climatic records in Meixian to represent the conditions in our study sites.

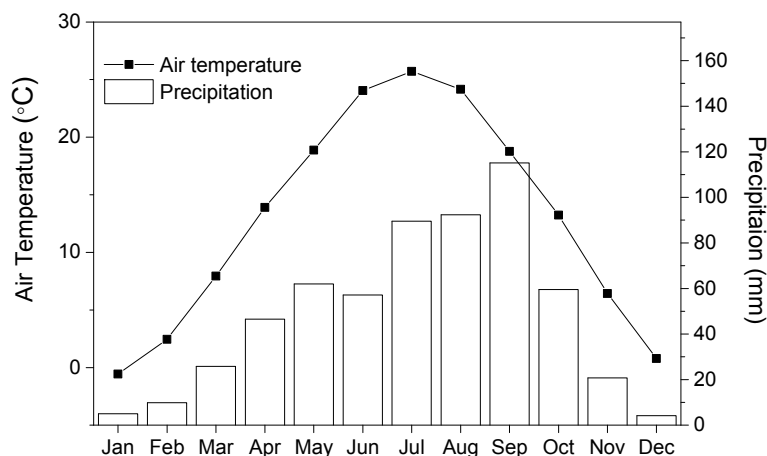


Figure 1. Monthly mean air temperatures and monthly precipitation based on the instrumental record from the meteorological station located in Meixian.

To assess climate trends in the Meixian record, we used the Kendall's tau coefficient (τ) and compared changes in seasonal variables (mean temperature, total precipitation) for two 28-year long sub-periods (1960–1987 vs. 1988–2015). We calculated the linear slopes of seasonal climatic variables for both sub-periods (DJF, winter; MAM, spring; JJA, summer; SON, autumn).

L. chinensis and *A. fargesii* are the dominant conifers in the study area, but they dominate at different elevations. *L. chinensis* grows from 2800 to 3500 m a.s.l. and forms the alpine treeline, whereas *A. fargesii* grows from 2400 to 3000 m. *A. fargesii* usually forms mixed stands with birch (*Betula albosinensis* Burkill) at a lower elevation, and with *L. chinensis* from 2800 to 3000 m, i.e., in the uppermost distribution limit of fir.

2.2. Tree-Ring Sampling and Chronology Development

A total of five sampling sites, with different elevations and dominated by the two species, were selected and sampled during 2014–2016. In total, 83 and 44 increment cores (one core per tree) were collected at 1.3 m using Pressler increment borers from healthy and dominant *L. chinensis* and *A. fargesii* trees, respectively. Tree-ring samples were processed following standard dendrochronological methods [24]. After a rigorous visual cross-dating of the tree-ring cores, ring widths were measured by using a Lintab 6 system with a resolution of 0.01 mm, and then the quality of the cross-dating was checked using the COFECHA program [25].

The tree-ring measurements were standardized to remove the biological growth trend by using a negative exponential functional function with the ARSTAN program [26]. Then, the resulting standard ring-width indices of each tree were averaged for each site using a biweight robust mean and no autoregressive modeling was performed. Therefore, we used the standard site chronologies in further analyses. However, to quantify growth trends, we used the τ statistic again for raw ring-width data considering the two 28-year long sub-periods examined for climate data (1960–1987 and 1988–2015).

Several descriptive statistics commonly used in dendrochronology were adopted to assess the variations in growth [27]. These statistics include: mean ring-width (MRW); standard deviation (SD); the mean sensitivity (MS), which quantifies the relative difference in width between consecutive rings; the first-order serial autocorrelation (AC), which assesses the serial persistence in growth; the mean inter-series correlation (RBAR); the signal-to-noise ratios (SNR); the variance accounted for by the first principle component (PC1); and the expressed population signal (EPS).

2.3. Spatial- and Species-Specific Analyses of Tree-Ring Width Chronologies

Principal component analysis (PCA) was used to detect relationships among the five standard chronologies over the common period from 1920 to 2015. The PCA was calculated on the covariance

matrix of the chronologies and only the two principal components (PC1 and PC2) were retained because they had an eigenvalue greater than one.

2.4. Relationships between Tree Growth and Climate

The influence of climate factors on the annual growth of forests was investigated by correlating (using Pearson coefficients) tree-ring width standard chronologies with monthly mean temperatures and precipitation records obtained from the Meixian meteorological station. Considering the lag effect of climate on tree growth, the selected climate variables encompassed from June of the previous year up to October of the current year over the period 1960–2015. To assess if climate-growth relationships changed through time, we also calculated correlations for two 28-year long sub-periods (1960–1987 and 1988–2015).

3. Results

3.1. Climate Trends

Climate in the study area has been characterized by warmer conditions since 1988 (Figure 2). Spring ($\tau = 0.65$, $p < 0.001$), summer ($\tau = 0.28$, $p = 0.04$), and autumn ($\tau = 0.26$, $p = 0.05$) temperatures have significantly risen during the last 28 years. However, significant cooling was observed for summer from 1967 to 1987 ($\tau = -0.52$, $p < 0.001$). In contrast, precipitation has not shown any significant trend.

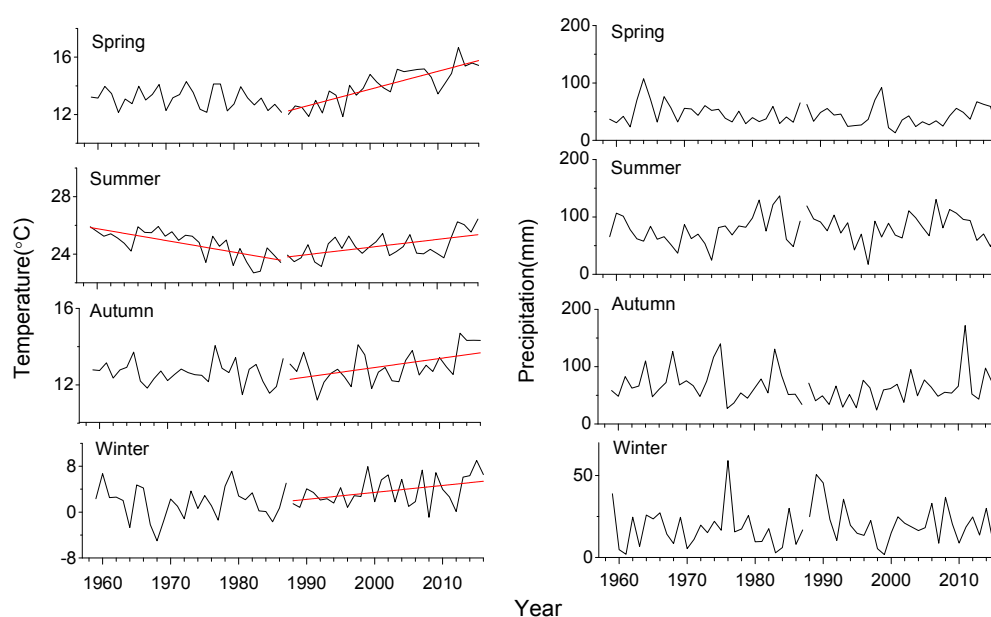


Figure 2. Trends in the seasonal temperature and precipitation values from 1960 to 2015 in Meixian. Lines indicate significant trends for two 28-year long sub-periods (1960–1987 and 1988–2015).

3.2. Characteristics of the Tree-Ring Width Chronologies

As shown in Table 1, *L. chinensis* has a narrower ring width (0.64 mm) and higher MS and RBAR than *A. fargesii* (0.83 mm). In contrast, *L. chinensis* has a lower AC than *A. fargesii* (Table 1). Similar high- to mid-frequency variability was observed in the standard chronologies of the same species sampled at different elevations (Figures 3a and 4). From 1960 to 1987, only *A. fargesii* at 3065 m showed a significant decline in growth ($\tau = -0.40$, $p = 0.003$) (Figure 3b). However, from 1988 to 2015, it was the *A. fargesii* stand located at 2860 m which showed a negative growth trend ($\tau = -0.34$, $p = 0.011$), whereas the *L. chinensis* forest located at 3080 m showed a positive growth trend ($\tau = 0.52$, $p < 0.001$).

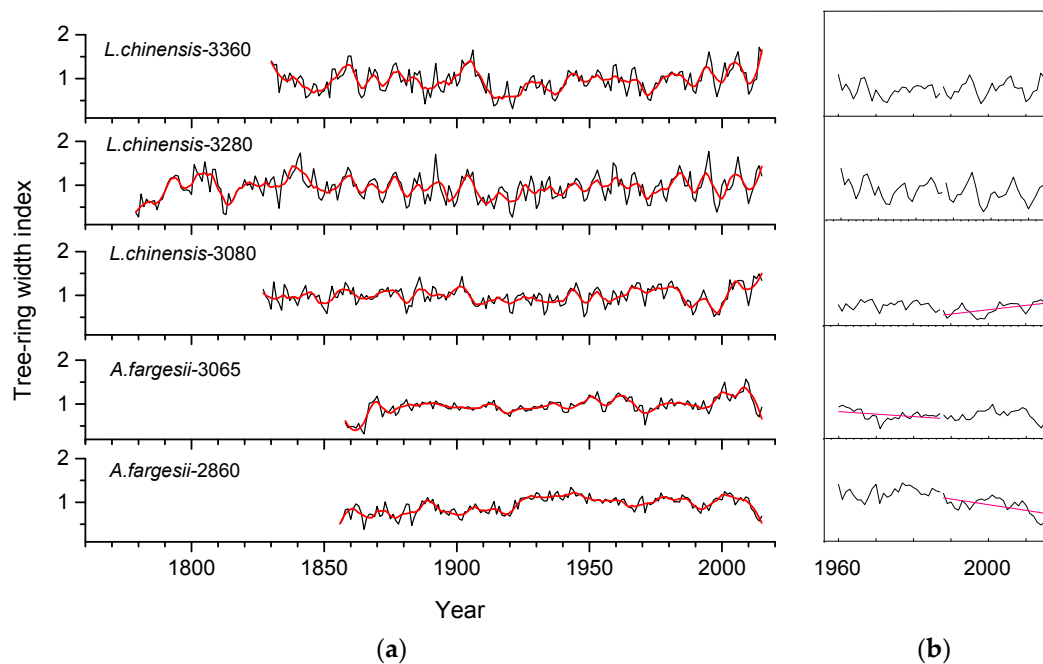


Figure 3. Indexed tree-ring width standard chronologies (a) of *L. chinensis* (larix) and *A. fargesii* (fir) along the elevational gradient and (b) corresponding tree-ring width data (in mm) since 1960 (plots displayed within the box). In the plot (a) thin (black) and bold (red) lines indicate annual values and 10-year moving averages, respectively. Numbers indicate the elevation (in m) of sampled stands. In plot (b) the red lines indicate significant ($p < 0.05$) trends of tree-ring width.

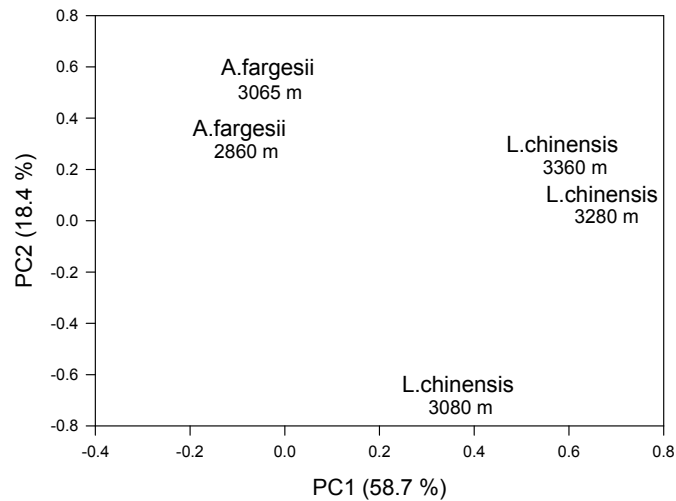


Figure 4. Loadings of the first and second principal components (PC1 and PC2) calculated on the covariance matrix of the five standard tree-ring width chronologies shown in Figure 3a and considering the common 1920–2015 period. Numbers indicate the forest elevations.

Table 1. Site information and dendrochronological statistics of the standard tree-ring width chronologies.

Species	Elevation (m)	Aspect	No. Trees	Age at 1.3 m (Years)	MS	Rbar	AC	EPS > 0.85 since.	Period 1950–2015				
									Mean TRW (mm)	Rbar	EPS	SNR	PC1 (%)
<i>L. chinensis</i>	3360	E	29	100	0.22	0.48	0.55	1910	0.66	0.51	0.96	26.4	54.1
	3280	E	29	130	0.24	0.31	0.58	1855	0.76	0.43	0.96	21.3	46.2
	3080	NE	25	135	0.17	0.38	0.52	1880	0.50	0.42	0.94	15.1	45.5
<i>A. fargesii</i>	3065	NE	21	115	0.15	0.28	0.77	1950	0.63	0.35	0.90	9.16	39.4
	2860	NW	23	90	0.14	0.28	0.73	1935	1.03	0.23	0.82	4.47	29.6

Abbreviations of variables: MS, mean Sensitivity; Rbar, mean inter-series correlations; AC, first-order autocorrelation; EPS, Expressed Population Signal; TRW, tree-ring width; SNR, Signal-to-Noise Ratio; PC1, first principal component.

The PC loadings clearly showed the separation of the five chronologies into two groups. The first principal component (PC1) yielded different loadings for the *L. chinensis* sites, particularly the two forest sites located at the highest elevation, and *A. fargesii* sites, whereas the second principal component (PC2) separated the low-elevation *L. chinensis* site with negative loadings from the rest of the sites (Figure 4). Such grouping matches the observed annual and decadal variability of ring-width indices observed in *L. chinensis* and *A. fargesii* standard chronologies (Figure 3a).

A high percentage of variation in the ring-width indices was accounted for by the PC1 (58.7%), confirming that *L. chinensis* growth reflected a more common and stronger climatic signal than *A. fargesii*, whilst the PC2 accounted for 18.4% of the total variation of these indices (Figure 4). This result could also be inferred by the higher values of Rbar, SNR, EPS, and PC1 observed in *L. chinensis* chronologies, which increased as elevation also rose (Table 1).

3.3. Topographic and Species-Related Influences on Growth Responses to Climate

The growth of *L. chinensis* and *A. fargesii* showed different responses to climate (Figure 5). In *L. chinensis*, ring-width indices were positively correlated with March to July temperatures of year of tree-ring formation and showed a reinforced association in 1988–2015. Warm previous August and current-January were negatively associated with growth in 1960–1987. Notably, the significant growth-temperature relationships in the pre-growing season appeared much earlier in the lower elevation. Wet April to June conditions were negatively related to growth.

The chronology of *A. fargesii* was negatively correlated with current July–August temperature. The chronology of *A. fargesii* at 2860 m was much more sensitive to July–August temperatures. Wet current-April conditions were negatively associated with *A. fargesii* growth, but precipitation July to August precipitation showed positive correlations with *A. fargesii* growth.

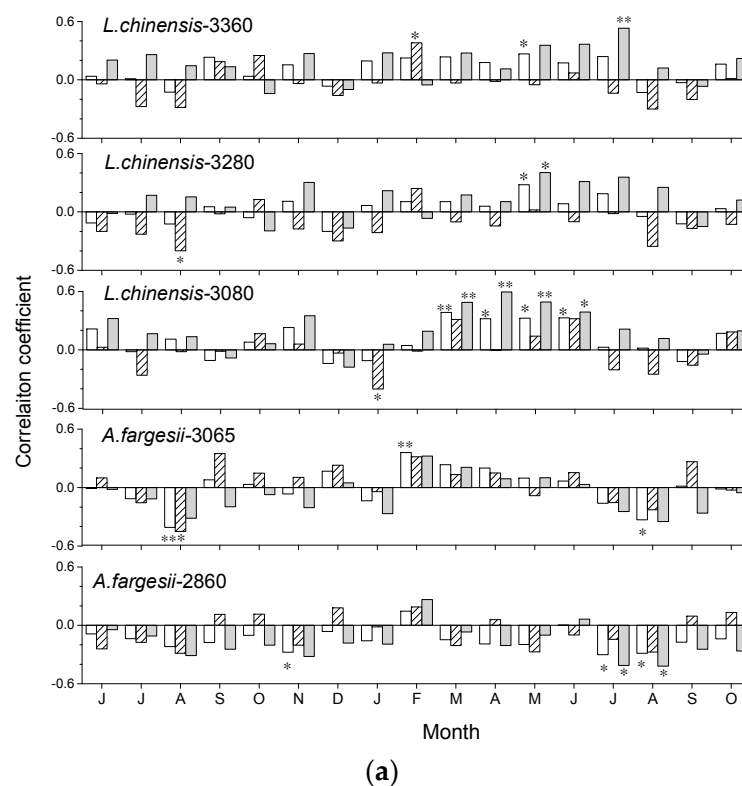


Figure 5. Cont.

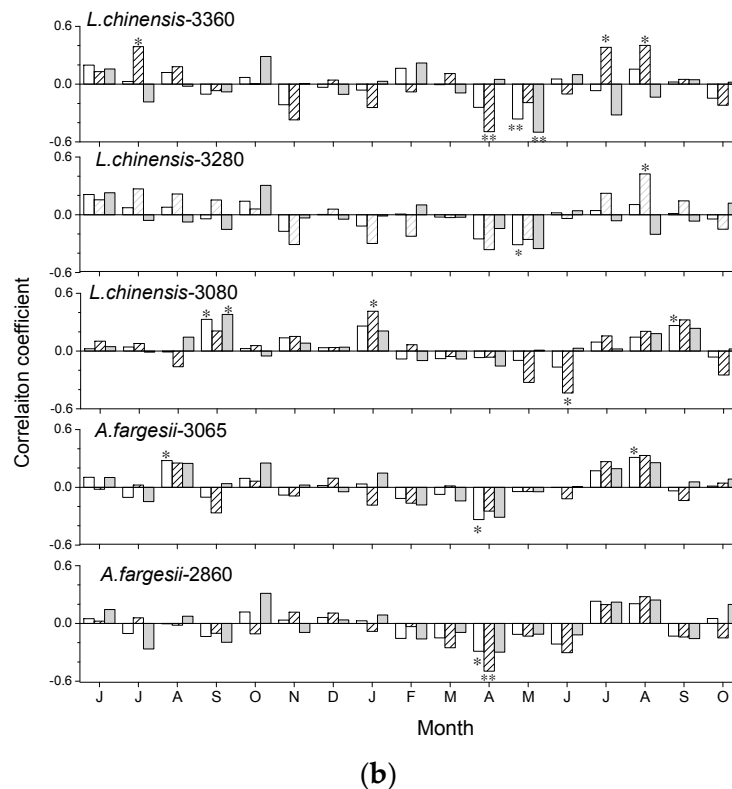


Figure 5. Correlations (* $p < 0.05$, ** $p < 0.01$) obtained by relating the standard tree-ring width chronologies of *Larix chinensis* and *Abies fargesii* with monthly mean temperature (a) and precipitation (b) along the site elevations. Climate variables go from the June of the previous year to current October of the year of tree-ring formation. Empty bars, hatched bars, and solid grey bars correspond to the 1960–2015, 1960–1987, and 1988–2015 periods, respectively.

4. Discussion

The dendrochronological statistics suggested a stronger coherence and climatic influence on *L. chinensis* growth at higher elevations than *A. fargesii* at lower elevations. Regardless of tree species, several statistics (MS, Rbar, EPS, and PC1) of the standard tree-ring chronologies increased with increasing elevation, indicating a higher year-to-year variability in growth and a more marked responsiveness to climate upwards. Similar values for these statistics have been reported in other mountain areas subjected to temperate and humid climate conditions [28]. This pattern is likely related to increasingly harsher environmental conditions such as a shorter growing season with increasing elevation as air and soil temperatures decrease [29].

Trees growing at higher elevations are more sensitive to temperature, while trees growing at lower elevations are usually more sensitive to precipitation and moisture availability during the boreal growing season (spring, summer). Similar findings were also reported in the Qinling Mountains [30] and central Hengduan Mountains [31]. However, our findings do not agree with studies under a similar sub-humid climate in the southeast Tibetan Plateau, which showed a common regional climatic signal (summer temperature) along the studied elevation gradients [32,33]. In our study, *L. chinensis* growth was favored by warmer conditions prior to the growing season but also during the spring of the growth year, whereas *A. fargesii* growth negatively responded to warm and dry summer conditions. The responses of *L. chinensis* correspond to a direct control of temperatures on radial growth through xylogenesis, as in other treeline-forming species, but may also be explained by a higher synthesis of carbohydrates during the previous autumn and winter [29,34–37]. Warmer spring temperatures would advance the onset of growing season by increasing the melting of snow cover and warming soil and stem meristems at higher elevations [35]. However, at lower elevations, a higher growing season

temperature could negatively impact the growth of *A. fargesii* through enhanced evapotranspiration leading to drought stress and reducing the rate of cambium division during xylogenesis [38,39], as has been described in drought-prone mountain forest environments [40,41]. Notably, the precipitation showed an earlier (April) and stronger negative impact on the growth of *A. fargesii* than *L. chinensis* in the pre-growing season. This result is probably due to the earlier start of the growing season of *A. fargesii*, and heavy precipitation could negatively impact the vitality through lowering the temperature, resulting in injuries to needles and shoots, or even damaging cambial tissues [42].

We also found different species-dependent growth responses to the warmer climate conditions observed in the study area. The growth of *L. chinensis* has benefitted from the spring warming detected since 1986, but we only detected a significant growth enhancement at the lowest elevation. It may be related to an earlier start of the growing season. However, the growth of *A. fargesii* at its low-elevation margin has declined in association with this warming, suggesting greater drought stress, possibly through increased vapor pressure deficit [43] given that precipitation did not decrease. Climate warming can cause an earlier start of the growing season in mid to high elevations, thus increasing radial-growth rates of the cold-tolerant *L. chinensis*, but warmer conditions can increase drought severity and lead to reduced growth at low elevations of the drought-intolerant *A. fargesii*. Such elevation- and species-related growth responses were also reported in other mountain areas subjected to multiple climatic influences along elevational gradients [44]. We speculate that climate warming could negatively influence the growth and productivity of *A. fargesii* forests at mid to low elevations, whereas a warmer spring temperature would favor *L. chinensis* growth.

5. Conclusions

Based on our characterization of changes in radial growth along a wide elevation gradient located in the Qinling Mountains, central China, we found that the growth responses to climate depended on tree species and site elevation. *L. chinensis* at high elevation showed a higher growth coherence between trees and responded more to climate than *A. fargesii* at low elevation. *L. chinensis* growth was favored by warm conditions prior to the growing season but also during the current growing season (spring), whereas *A. fargesii* growth was mainly limited by warm-dry summer conditions. The radial growth of *L. chinensis* shows an increasing trend at low elevation as spring temperatures rise, whereas the low-elevation *A. fargesii* forest shows a decreasing growth trend. Thus, climate warming could favor *L. chinensis* growth but make low-elevation *A. fargesii* forest more vulnerable to water shortage.

Author Contributions: B.L. and E.L. performed field sampling and tree-ring measurements; B.L. and J.J.C. performed most statistical analyses; B.L., E.L., K.L., and J.J.C. led the writing of the paper and contributed to data interpretation.

Funding: This work was funded by the National Natural Science Foundation of China (41601192 and 41525001), and China Postdoctoral Science Foundation (2015M572591). J.J.C. thanks the support of the CGL2015-69186-C2-1-R project (Spanish Ministry of Economy).

Acknowledgments: We thank Qingsong Du for assistance in fieldwork.

Conflicts of Interest: The authors declare no conflict of interest

References

1. Bonan, G.B. Forests and climate change: Forcings, feedbacks, and the climate benefits of forests. *Science* **2008**, *320*, 1444–1449. [[CrossRef](#)] [[PubMed](#)]
2. Allen, C.D.; Breshears, D.D.; McDowell, N.G. On underestimation of global vulnerability to tree mortality and forest die-off from hotter drought in the anthropocene. *Ecosphere* **2015**, *6*, 1–55. [[CrossRef](#)]
3. Liu, H.; Williams, A.P.; Allen, C.D.; Guo, D.; Wu, X.; Anenkhonov, O.A.; Liang, E.; Sandanov, D.V.; Yin, Y.; Qi, Z.; et al. Rapid warming accelerates tree growth decline in semi-arid forests of Inner Asia. *Glob. Chang. Biol.* **2013**, *19*, 2500–2510. [[CrossRef](#)] [[PubMed](#)]
4. Fang, O.; Alfaro, R.I.; Zhang, Q.B. Tree rings reveal a major episode of forest mortality in the late 18th century on the Tibetan Plateau. *Glob. Planet. Chang.* **2018**, *163*, 44–50. [[CrossRef](#)]

5. Zhang, Q.B.; Evans, M.N.; Lyu, L. Moisture dipole over the Tibetan Plateau during the past five and a half centuries. *Nat. Commun.* **2015**, *6*, 8062. [[CrossRef](#)] [[PubMed](#)]
6. Liang, E.; Leuschner, C.; Dulamsuren, C.; Wagner, B.; Hauck, M. Global warming-related tree growth decline and mortality on the north-eastern Tibetan Plateau. *Clim. Chang.* **2016**, *134*, 163–176. [[CrossRef](#)]
7. Salzer, M.W.; Hughes, M.K.; Bunn, A.G.; Kipfmüller, K.F. Recent unprecedented tree-ring growth in bristlecone pine at the highest elevations and possible causes. *Proc. Natl. Acad. Sci. USA* **2009**, *106*, 20348–20353. [[CrossRef](#)] [[PubMed](#)]
8. Liang, E.; Shao, X.; Xu, Y. Tree-ring evidence of recent abnormal warming on the southeast Tibetan Plateau. *Theor. Appl. Climatol.* **2009**, *98*, 9–18. [[CrossRef](#)]
9. Littell, J.S.; Peterson, D.L.; Tjoelker, M. Douglas-fir growth in mountain ecosystems: Water limits tree growth from stand to region. *Ecol. Monogr.* **2008**, *78*, 349–368. [[CrossRef](#)]
10. Chen, D.; Fang, K.; Li, Y.; Dong, Z.; Zhang, Y.; Zhou, F. Response of *Pinus taiwanensis* growth to climate changes at its southern limit of Daiyun Mountain, mainland China Fujian Province. *Sci. China-Earth Sci.* **2016**, *59*, 328–336. [[CrossRef](#)]
11. Camarero, J.J.; Fajardo, A. Poor acclimation to current drier climate of the long-lived tree species *Fitzroya cupressoides* in the temperate rainforest of southern Chile. *Agric. For. Meteorol.* **2017**, *239*, 141–150. [[CrossRef](#)]
12. Ashton, M.S.; Tyrrell, M.L.; Spalding, D.; Gentry, B. *Managing Forest Carbon in a Changing Climate*; Springer: New York, NY, USA, 2012.
13. Blois, J.L.; Williams, J.W.; Fitzpatrick, M.C.; Jackson, S.T.; Ferrier, S. Space can substitute for time in predicting climate-change effects on biodiversity. *Proc. Natl. Acad. Sci. USA* **2013**, *110*, 9374–9379. [[CrossRef](#)] [[PubMed](#)]
14. Elmendorf, S.C.; Henry, G.H.R.; Hollister, R.D.; Fosaa, A.M.; Gould, W.A.; Hermanutz, L.; Hofgaard, A.; Jónsdóttir, I.S.; Jorgenson, J.C.; Lévesque, E.; et al. Experiment, monitoring, and gradient methods used to infer climate change effects on plant communities yield consistent patterns. *Proc. Natl. Acad. Sci. USA* **2015**, *112*, 448–452. [[CrossRef](#)] [[PubMed](#)]
15. Qi, Z.; Liu, H.; Wu, X.; Hao, Q. Climate-driven speedup of alpine treeline forest growth in the Tianshan Mountains, northwestern China. *Glob. Chang. Biol.* **2015**, *21*, 816–826. [[CrossRef](#)] [[PubMed](#)]
16. Bayramzadeh, V.; Zhu, H.; Lu, X.; Attarod, P.; Zhang, H.; Li, X.; Asad, F.; Liang, E. Temperature variability in northern Iran during the past 700 years. *Sci. Bull.* **2018**, *63*, 462–464. [[CrossRef](#)]
17. Hartl-Meier, C.; Dittmar, C.; Zang, C.; Rothe, A. Mountain forest growth response to climate change in the Northern Limestone Alps. *Trees* **2014**, *28*, 819–829. [[CrossRef](#)]
18. Zimmermann, J.; Hauck, M.; Dulamsuren, C.; Leuschner, C. Climate warming-related growth decline affects *Fagus sylvatica*, but not other broad-leaved tree species in central European mixed forests. *Ecosystems* **2015**, *18*, 560–572. [[CrossRef](#)]
19. Zhang, X.; Liu, X.; Zhang, Q.; Zeng, X.; Xu, G.; Wu, G.; Wang, W. Species-specific tree growth and intrinsic water-use efficiency of Dahurian larch (*Larix gmelinii*) and Mongolian pine (*Pinus sylvestris* var. *Mongolica*) growing in a boreal permafrost region of the greater Hinggan Mountains, northeastern China. *Agric. For. Meteorol.* **2018**, *248*, 145–155.
20. Dang, H.; Zhang, Y.; Zhang, K.; Jiang, M.; Zhang, Q. Age structure and regeneration of subalpine fir (*Abies fargesii*) forests across an altitudinal range in the Qinling Mountains, China. *For. Ecol. Manag.* **2010**, *259*, 547–554. [[CrossRef](#)]
21. Liu, Y.; Linderholm, H.W.; Song, H.; Cai, Q.; Tian, Q.; Sun, J.; Chen, D.; Simelton, E.; Seftigen, K.; Tian, H.; et al. Temperature variations recorded in *Pinus tabulaeformis* tree rings from the southern and northern slopes of the central Qinling mountains, central China. *Boreas* **2009**, *38*, 285–291. [[CrossRef](#)]
22. Jiang, C.; Mu, X.; Wang, F.; Zhao, G. Analysis of extreme temperature events in the Qinling Mountains and surrounding area during 1960–2012. *Quat. Int.* **2016**, *392*, 155–167. [[CrossRef](#)]
23. Chen, F.; Zhang, R.; Wang, H.; Qin, L. Recent climate warming of central China reflected by temperature-sensitive tree growth in the eastern Qinling Mountains and its linkages to the Pacific and Atlantic oceans. *J. Mt. Sci.* **2015**, *12*, 396–403. [[CrossRef](#)]
24. Cook, E.; Kairiukstis, L. *Methods of Dendrochronology: Applications in the Environmental Sciences*; Kluwer: Dordrecht, The Netherlands, 1990.
25. Holmes, R.L. Computer-assisted quality control in tree-ring dating and measurement. *Tree-Ring Bull.* **1983**, *43*, 69–75.

26. Cook, E. A time-Series Analysis Approach to Tree Ring Standardization. Ph.D. Thesis, University of Arizona, Tucson, AZ, USA, 1985.
27. Fritts, H.C. *Tree Rings and Climate*; Blackburn Press: Caldwell, ID, USA, 2001.
28. Splachtna, B.E.; Dobry, J.; Klinka, K. Tree-ring characteristics of subalpine fir (*Abies lasiocarpa* (hook.) nutt.) in relation to elevation and climatic fluctuations. *Ann. For. Sci.* **2000**, *57*, 89–100. [[CrossRef](#)]
29. Körner, C. *Alpine Treelines: Functional Ecology of the Global High Elevation Tree Limits*; Springer: Basel, Switzerland, 2012.
30. Dang, H.; Jiang, M.; Zhang, Q.; Zhang, Y. Growth responses of subalpine fir (*Abies fargesii*) to climate variability in the Qinling Mountain, China. *For. Ecol. Manag.* **2007**, *240*, 143–150. [[CrossRef](#)]
31. Fan, Z.; Bräuning, A.; Cao, K.; Zhu, S. Growth-climate responses of high-elevation conifers in the central Hengduan Mountains, southwestern China. *For. Ecol. Manag.* **2009**, *258*, 306–313. [[CrossRef](#)]
32. Liang, E.; Wang, Y.; Xu, Y.; Liu, B.; Shao, X. Growth variation in *Abies georgei* var. *smithii* along altitudinal gradients in the Sygera Mountains, southeastern Tibetan Plateau. *Trees* **2010**, *24*, 363–373.
33. Liu, B.; Wang, Y.; Zhu, H.; Liang, E.; Camarero, J.J. Topography and age mediate the growth responses of Smith fir to climate warming in the southeastern Tibetan Plateau. *Int. J. Biometeorol.* **2016**, *60*, 1577–1587. [[CrossRef](#)] [[PubMed](#)]
34. Wang, Y.; Liang, E.; Sigdel, S.; Liu, B.; Camarero, J.J. The coupling of treeline elevation and temperature is mediated by non-thermal factors on the Tibetan Plateau. *Forests* **2017**, *8*, 109. [[CrossRef](#)]
35. Rossi, S.; Deslauriers, A.; Anfodillo, T.; Carraro, V. Evidence of threshold temperatures for xylogenesis in conifers at high altitudes. *Oecologia* **2007**, *152*, 1–12. [[CrossRef](#)] [[PubMed](#)]
36. Li, X.; Liang, E.; Gričar, J.; Rossi, S.; Čufar, K.; Ellison, A.M. Critical minimum temperature limits xylogenesis and maintains treelines on the southeastern Tibetan Plateau. *Sci. Bull.* **2017**, *62*, 804–812. [[CrossRef](#)]
37. Liang, E.; Camarero, J.J. Threshold-dependent and non-linear associations between temperature and tree growth at and below the alpine treeline. *Trees* **2018**, *32*, 661–662. [[CrossRef](#)]
38. Ren, P.; Rossi, S.; Camarero, J.J.; Ellison, A.M.; Liang, E.; Peñuelas, J. Critical temperature and precipitation thresholds for the onset of xylogenesis of *Juniperus przewalskii* in a semi-arid area of the north-eastern Tibetan Plateau. *Ann. Bot.* **2018**, *121*, 617–624. [[CrossRef](#)] [[PubMed](#)]
39. Ziaco, E.; Truettner, C.; Biondi, F.; Bullock, S. Moisture-driven xylogenesis in *Pinus ponderosa* from a Mojave Desert mountain reveals high phenological plasticity. *Plant Cell Environ.* **2018**, *41*, 823–836. [[CrossRef](#)] [[PubMed](#)]
40. Zhang, L.; Jiang, Y.; Zhao, S.; Jiao, L.; Wen, Y. Relationships between tree age and climate sensitivity of radial growth in different drought conditions of Qilian Mountains, northwestern China. *Forests* **2018**, *9*, 135. [[CrossRef](#)]
41. Gao, L.; Gou, X.; Deng, Y.; Liu, W.; Yang, M.; Zhao, Z. Climate–growth analysis of Qilian juniper across an altitudinal gradient in the central Qilian Mountains, northwest China. *Trees* **2013**, *27*, 379–388. [[CrossRef](#)]
42. Gurskaya, M.; Shiyatov, S. Distribution of frost injuries in the wood of conifers. *Russ. J. Ecol.* **2006**, *37*, 7–12. [[CrossRef](#)]
43. Aussenac, G. Ecology and ecophysiology of circum-Mediterranean firs in the context of climate change. *Ann. For. Sci.* **2002**, *59*, 823–832. [[CrossRef](#)]
44. González-Cásares, M.; Pompa-García, M.; Camarero, J.J. Differences in climate–growth relationship indicate diverse drought tolerances among five pine species coexisting in northwestern Mexico. *Trees* **2017**, *31*, 531–544. [[CrossRef](#)]

